Comparison of Hemodynamic and Structural Indices of Ascending Thoracic Aortic Aneurysm as predicted by 2-way FSI, CFD Rigid Wall Simulation and Patient-Specific Displacement-Based FEA

Journal:	*Part H: Journal of Engineering in Medicine*
Manuscript ID	Draft
Manuscript Type:	Original article
Date Submitted by the Author:	n/a
Complete List of Authors:	Mendez, Vincent; Ecole Polythechnique Fédérale de Lausanne Di Giuseppe, Marzio; Fondazione RiMED Pasta, Salvatore
Keywords:	Cardiovascular System Mechanics, Clinical Outcome Prediction, Finite Element Modelling/ Analysis [Medical], Haemodynamics Modelling, Finite Element [Biomechanics]
Abstract:	Patient-specific computational modeling is increasingly being used to predict structural and hemodynamic parameters, especially when current clinical tools are not accessible. In this contest, pathophysiology of ascending thoracic aortic aneurysm (ATAA) has been simulated to quantify patient risk by novel prognostic parameters and thus to improve the clinical decision-making process related to the intervention of ATAAs. In this study, the relevance of aneurysmal wall elasticity in determining parameters of clinical importance, such as shear stress, is discussed together with the significance of applying realistic boundary conditions to consider the aortic stretch and twist transmitted by the heart motion. Results from both finite element analysis (FEA) and computational fluid-dynamic (CFD) were compared to those of 2-way fluid-solid interaction analyses (FSI), which were carried out on ATAAs with either bicuspid aortic valve (BAV) or tricuspid aortic valve (TAV). Although the spatial distribution of wall shear (WSS) and intramural stresses (IMS) differed for a given ATAA, correlation analysis and Bland-Altman plots demonstrated that CFD-related WSS and FEA-related IMS predictions were comparable with those derived by a more sophisticated 2-way FSI modeling. This is likely caused by the stiff aneurysmal wall showing reduced diameter changes over cardiac beating (ie, 4.2±2.4%). Therefore, with the fact that there is no gold-standard for the assessment of hemodynamic and structural mechanics of ATAAs and with accepted limitations of our approach, computational technique has to be verified before applications in routine clinical practice as demonstrated in this study.

Comparison of Hemodynamic and Structural Indices of Ascending Thoracic Aortic Aneurysm as predicted by 2-way FSI, CFD Rigid Wall Simulation and Patient-Specific Displacement-Based FEA

Vincent Mendez[1], Marzio Di Giuseppe[2], Salvatore Pasta[2,3]

[1] Ecole Polythechnique Fédérale de Lausanne (EPFL), Switzerland

[2] Fondazione Ri.MED, Palermo, Italy;

[3] Department for the Treatment and Study of Cardiothoracic Diseases and Cardiothoracic Transplantation, IRCCS-ISMETT, Palermo, Italy

Corresponding author:

Salvatore Pasta, PhD

NSQ Professor in Industrial Bioengineering,

Fondazione Ri.MED

Phone: +39 091 3815681

FAX: +39 091 3815682

e-mail: spasta@fondazionerimed.com

Abstract:

Patient-specific computational modeling is increasingly being used to predict structural and hemodynamic parameters, especially when current clinical tools are not accessible. In this contest, pathophysiology of ascending thoracic aortic aneurysm (ATAA) has been simulated to quantify patient risk by novel prognostic parameters and thus to improve the clinical decision-making process related to the intervention of ATAAs. In this study, the relevance of aneurysmal wall elasticity in determining parameters of clinical importance, such as shear stress, is discussed together with the significance of applying realistic boundary conditions to consider the aortic stretch and twist transmitted by the heart motion. Results from both finite element analysis (FEA) and computational fluid-dynamic (CFD) were compared to those of 2-way fluid-solid interaction analyses (FSI), which were carried out on ATAAs with either bicuspid aortic valve (BAV) or tricuspid aortic valve (TAV). Although the spatial distribution of wall shear (WSS) and intramural stresses (IMS) differed for a given ATAA, correlation analysis and Bland-Altman plots demonstrated that CFD-related WSS and FEA-related IMS predictions were comparable with those derived by a more sophisticated 2-way FSI modeling. This is likely caused by the stiff aneurysmal wall showing reduced diameter changes over cardiac beating (ie, 4.2±2.4%). Therefore, with the fact that there is no gold-standard for the assessment of hemodynamic and structural mechanics of ATAAs and with accepted limitations of our approach, computational technique has to be verified before applications in routine clinical practice as demonstrated in this study.

Key words: ascending thoracic aortic aneurysm, fluid-solid interaction (FSI), finite element analysis (FEA), computational fluid-dynamic (CFD)

INTRODUCTION

An ascending thoracic aortic aneurysm (ATAA) is a life-threatening cardiovascular emergency with remarkable morbidity and mortality[1]. The incidence of ATAAs is 10/100,000 persons per year, occurring most commonly in the sixth and seventh decades of life and in men more frequently than women (ratio 3:1)[1]. Fatal complications such as aortic rupture or dissection are most commonly associated with ATAA development and progress, and these fatal outcomes can be prevented by surgical repair of dilated aorta. Davies et al [2] reported that rupture rates in patients not treated surgically range from 21% to 74% and that the risk of operation is relevant as well. Indeed, elective surgery carries a mortality rate of approximately 5%-9%, with value upon 57% for emergency surgery. Among risk factors predisposing individuals to aortic dilatation, bicuspid aortic valve (BAV) is the most relevant as the reported prevalence of dilatation of the ascending aorta among individuals with BAV (namely “bicuspid aortopathy”) ranges from 20 to 84% [3]. Individuals with BAV have higher prevalence of abnormal ascending aorta dilatation and 9-fold increased risk of aneurysm rupture than that of tricuspid aortic valve (TAV) [4].

Although the current clinical criterion based on the “maximum aortic diameter” can be adjusted by the body surface area to achieve higher patient specificity, progress is needed toward even better metrics and diagnostic tools to reliably distinguish the more from the less ‘malignant’ ATAA. Novel approaches should rely on sound physical principles rather than surgeon’s experience and clinical evidence to quantify the threat. For surveillance imaging and risk stratification strategies, computational modeling has been demonstrated to perform better than current clinical criterion of the aortic size for predicting the likelihood of abdominal aortic aneurysm failure [5]. Indeed, a potential tool to tailor patient-specific indications is to perform hemodynamic and aortic wall structural simulations to extrapolate indicators of aneurysm risk other than aortic size. Structural finite-element analyses (FEA) of aneurysmal wall stresses [6-10], computational fluid dynamics (CFD) of hemodynamic patterns dictated by aortic valve morphology (BAV vs TAV) [11-15], and 2-way fluid-solid interaction (FSI) simulations [16, 17] to account for multiphysics phenomena have been proposed, each modeling technique with advantage and disadvantages. In the majority of FEA the blood flow is simulated with a steady-state pressure boundary condition whereas CFD studies are based on a rigid wall assumption. FSI is therefore preferable but still a very complex task to handle and is computationally expensive. Most importantly, none of current computational studies reported in literature considered the longitudinal stretch and twist of the aortic wall induced by the heart beating as boundary conditions of FEA.

This study aims to assess whether simply FEA and CFD modeling would give similar predictions of structural and hemodynamic parameters as compared to 2-way FSI analyses of ATAAs. Thus, this work is focused on the ability of computational modeling to replicate aneurysm physiology in a less complex fashion as possible. Of course, we cannot claim that 2-way FSI simulation is the gold-standard, because there is no standard to compare against. Nevertheless, within the accepted limitations of our computational modeling approach, if large differences are observed in the hemodynamic and structural parameters between FEA/CFD model and 2-way FSI, one could raise a red flag for further investigation. Moreover, we profited from this work to improve our FEA approach by taking into consideration the patient-specific motion of ATAAs during cardiac beating as this was determined by *in-vivo* analysis of electrocardiogram-gated computed tomography angiographic data (ECG-gated CTA) [18].

METHODS

Study Population and Geometry

After internal review board approval and informed consent, 11 patients (4 BAV and 7 TAV) underwent aortic size evaluation by ECG-gated CTA were investigated by computational analysis. Specifically, ECG-gated CTA scans were reconstructed to obtain images at cardiac phases corresponding to both diastole and systole. None of investigated patients had greater than mild aortic stenosis or aortic regurgitation assessed by echocardiography. For each patient, reconstructions of the whole aorta were performed with the shape of aortic valve fully opened and totally closed using the software Mimics (Mimics v17, Materialise, Leuven, BE). The point cloud of ATAA geometry was triangulated to generate a stereolithographic surface mesh, which was then exported to ICEM CFD 14.0 (ANSYS Inc., Canonsburg, PA) to generate the mesh of the fluid (lumen) and structural (aneurysm wall) domains. Table 1 summarizes demographic and functional echocardiographic data, valve morphology and aortic diameters for each patient.

2-way FSI Analysis

Parallel coupled, 2-way FSI analyses were carried out using an approach previously developed by the authors' group to couple the structural component, ABAQUS v6.12 (SIMULIA Inc, Providence, RI), and the fluid solver, FLUENT v14.0.0 (ANSYS Inc., Canonsburg, PA) [16]. Coupling was done with the software MpCCI v4.2 (Fraunhofer SCAI, Germany), with FLUENT sending the fluid-induced wall forces to ABAQUS, and ABAQUS sending the deformed nodal coordinates to FLUENT. Both codes share the aortic wall surface as boundary surface for the data exchange.

For the structural model, ATAA wall was modeled by a fiber-reinforced structural model introduced by Gasser and collaborators with material and collagen properties derived from previously published experimental data [19]. The biomechanical behavior of the aorta was different for BAV patients than for TAV patients. Uniform material properties and thickness (1.8 mm for BAV and 2.0 mm for TAV) for the aortic wall were adopted. Distal ends of supra-aortic vessels, aortic valve and descending aorta were fixed in all directions. The luminal surface of ATAA was used to exchange data with FLUENT. Solution was obtained using Dynamic/Implicit formulation assuming a structural density of 1120 kg/m^3. Motion of the aortic valve was not simulated.

For the fluid model, transient-time solver with second order implicit time advanced scheme was used for the steady-state fluid dynamic simulation of the systolic peak. The blood flow was assumed laminar, incompressible and Newtonian with density of 1060 kg/m^3 and viscosity of 0.00371 Pa × s. Pressure-implicit with splitting of operators (PISO) and skewness correction as pressure–velocity coupling and pressure staggering option (PRESTO) scheme as pressure interpolation method with 2nd order accurate discretization were adopted. Convergence was enforced by reducing the residual of the continuity equation by 10^{-5} at every time step. To include patient-specific hemodynamics, the transaortic jet velocity evaluated by Doppler echocardiography was set as the inflow velocity condition at the aortic valve for each patient. The inlet flow was then split between supra-aortic vessels and descending aorta using resistances boundary conditions with values extrapolated from Kim and collaborators [20].

FEA/CFD Analysis

The FEA/CFD analyses of ATAA consisted of both a FEA analysis of the aortic wall from diastole to systole and a CFD study of the flow-dynamic over the cardiac cycle. To ensure the deformed shape of ATAA geometries was similar to that of CFD study, the loading condition of the structural model consisted of a displacement field that was determined by temporal tracking of aortic luminal surfaces using a mathematical algorithm developed previously [18]. Specifically, the point cloud of the aortic luminal surface reconstructed at diastole was projected normally onto the aortic surface reconstructed at the systolic phase. The relative displacement of the aortic wall was evaluated as the Euclidean distance between reference and projected points. The estimated diastolic-to-systolic displacement of ATAA wall was used as boundary condition in the FEA simulation to obtain the stress distribution. This allowed us to consider the effect of the stretch and twist due to cardiac beating on the final ATAA deformed shape since this was complex to be simulated by 2-way FSI.

For the FEA, the ATAA model setup was similar to that of 2-way FSI in terms of constitutive formulation, material properties and tissue thickness. As boundary conditions, the diastolic-to-systolic displacement field of ATAA found for each vertex of the point ATAA cloud was interpolated on the closest node of the structural mesh.

For the CFD, we carried out unsteady simulations of the entire cardiac cycle with the aortic valve fully-opened and a rigid ATAA wall as reconstructed at systole. The waveform of the inlet flow velocity was extrapolated from phase-contrast magnetic resonance (MR) data with the peak scaled to match the transaortic jet velocity measurement of each patient [12]. This inflow was split between the supra-aortic vessels and the descending aorta using resistance boundary conditions as described for the 2-way FSI modeling. The cardiac cycle was split in ten phases, and simulations were continued through two cardiac cycles to eliminate non-linear startup effects. Results presented here were obtained at the last cycle. Laminar condition, fluid material properties and pressure–velocity coupling algorithm were equal to that of 2-way FSI.

Structural and Hemodynamic Variables and Statistical Analysis

The following hemodynamic and structural variables for each analysis were extrapolated at systolic peak and then compared between FEA/CFD analyses and 2-way FSI. Specifically, the pressure index (PI) was determined as the mean of 95% higher values of pressure normalized by the peak; the helical flow index (HFI) as descriptor of the complex, fully three dimensional flow fields as described by Morbiducci et al. (this variable as a range of $0 \le HFI \le 1$ with 0 for irrotational flow) [21]; the intramural stress (IMS) in term of Von Mises stress; and the peak systolic wall shear stress (WSS). All variables were measured at three different regions of the aorta: the sino-tubular junction (STJ), the mid-ascending aorta (AA middle) and the distal ascending aorta (AA distal). These variables were processed using EnSight software package (EnSight v10.0.1(b), CEI, Apex, NC).

All continuous descriptive data are expressed as mean ± SD. Bland–Altman plots were graphed to establish the degree of concordance and agreement between FEA/CFD analyses and 2-way FSI. The association between each variable was explored using Pearson and Spearman's correlation coefficients. Statistical analyses were performed using SPSS software (IBM SPSS Statistics, Armonk, NY, USA). All probability values were considered significant for $p<0.05$.

RESULTS

Figure 1 shows that flow streamlines derived by CFD analyses were parallels with minimal deviance from the initial direction of the aortic-valve flow for TAV ATAAs and helical within the ascending aorta of BAV ATAAs. These patterns were similar with respect to 2-way FSI counterparts (results not shown). We observed differences in the spatial distribution of the WSS at peak of systole between CFD and 2-way FSI. Figure 2 shows maxima of CFD-related WSS in the ascending aorta of ATAAs while FSI-related shear stress appeared highest in the distal ascending aorta (see Figure 6). For FEA, the IMS highlighted differences in the spatial distribution of local maxima that are mainly located at the aortic root in the major curvature of aneurysmal aorta as compared to 2-

way FSI counterparts (Figure 3). For two representative patients with BAV ATAA and TAV ATAA (see Figure 6), FSI-related IMS presented maxima in the region of the minor curvature of the aneurysmal aorta. Global indexes of the hemodynamic environment of the entire ascending aorta (see Figure 4) evinced that the mean value of HFI does not differ between 2-way FSI and CFD analyses, and that the mean value of the CFD-related PI is statistically significant lower than that of 2-way FSI (p=0.005). At Pearson and Spearman correlation analyses, there were no statistical differences in the hemodynamic and structural indexes between FEA/CFD and 2-way FSI at the anatomic regions of STJ, middle and distal ascending aorta (see Table 2 and 3). Similarly, Bland–Altman analysis demonstrated a good agreement in the peak value of the investigated hemodynamic and structural indexes estimated by either FEA or CFD with respect to 2-way FSI counterparts for each of anatomic locations (Figure 5).

DISCUSSION

In this study, we compared hemodynamic and structural parameters estimated with both a FEA and CFD analyses of patient-specific ATAA models with those determined by 2-way FSI analyses. This allowed us to assess the relevance of aneurysmal wall compliance in determining parameters of clinical importance for risk stratification of ATAA failure and thus to understand whether one complex 2-way FSI approach can be replaced by two more simple FEA and CFD studies. The most striking finding is that the stiff ATAA wall structure leads to unremarkable changes in the WSS predictions between CFD and 2-way FSI and that patient-specific displacement-based boundary conditions revealed a dissimilar distribution of IMS when compared to the flow-induced loading condition of FSI modeling.

Effect of wall elasticity was studied in cerebral aneurysm by Torii and collaborators [22] and showed similar results to those here presented. For a given patient, the WSS distribution is different between FSI and rigid wall simulations (Figure 6), meaning that temporal gradients in WSS would be different, especially in the ascending aorta. Using FEA and FSI modeling, Reymond and collaborators [23] demonstrated that the WSS-related difference between FSI and CFD becomes relevant when the aortic diameter change between diastole and systole reaches 10–15%. They also found that the relatively less compliant descending thoracic aorta shows comparable shear stress between FSI and rigid wall simulation. In our patient study group, the diameter change over the cardiac cycle was 4.2±2.4% because of the stiff aneurysmal wall structure inhibiting aortic expansion. This may explain the relative lesser difference in the WSS predictions between CFD and 2-way FSI analyses as demonstrated by correlation and Bland–Altman plots (Figure 5). Although differences exists in the spatial distribution of the shear stress among modeling techniques, CFD analysis of ATAAs appears reliable and does not present numerical instabilities due to the coupling/constraint with the structural solver as in FSI.

With regards to the structural analysis, different distributions were found for the IMS exerted on the aneurysmal wall by the displacement-based FEA versus the flow-induced 2-way FSI analysis of ATAAs because of boundary condition approaches adopted in each of computational techniques. This finding hampers us to make any conclusion on the benefit of FEA. While the 2-way FSI simulation taken into account the frictional component induced by the moving fluid on the aneurysmal wall, the IMS distribution shown by our FEA considered the effect of the heart motion (ie, stretch and twist) on the ATAA mechanics. To our knowledge, this approach has never been reported. Indeed, using FEA of ATAAs loaded at uniform pressure of 120 mmHg, Nathan et al. [6] demonstrated that the aneurysmal wall has local maxima of IMS above the STJ on either the major or minor curvature of the ascending aorta. Later, they demonstrated that ATAA with BAV exhibited increased IMS above the STJ more often than TAV patients, and increased rupture risk with elevated systolic IMS and tissue stiffness [7]. However, nearly 60% of local maxima of IMS reported by Nathan et al. [7] are located in the minor curvature of the aorta while most of rupture and dissection are clinically seen along the greater curvature of the aorta. Similar locations of IMS maxima were reported by the totality of FEA studies documented in literature [6-10, 16], thereby suggesting inaccurate representation of ATAA physiology when the true aortic motion is not simulated. Our results using FEA analysis with patient-specific displacement-based boundary conditions highlighted that ATAA does not only expand due to the effect of blood pressure but also moves from diastole to the systole by influencing the IMS distribution. The force driving the aortic annulus motion is the ventricular traction accompanying cardiac beating and is transmitted to the aortic root and the ascending aorta. Thus, the aortic root motion has a direct influence on the deformation of the aorta and on the mechanical stress exerted on the aortic wall. Using cine-MR imaging and FEA analysis, Belller et al. [24] quantified the aortic root motion in healthy individuals and then carried out a FEA to assess the influence of the aortic root movement on the risk of aortic dissection. The longitudinal stress was found to increase remarkably in the major curvature of the ascending aorta, suggesting increased risk of dissection in this area. It should be highlighted that root motion alone is only an indicator of the force that the heart exerts on the aorta. Thus, a large aortic root displacement may be well tolerated in a compliant healthy aorta or may cause a disaster in a subject with stiffer aortic tissue as that induced by the presence of ATAA disease.

The best approach would be to integrate the patient-specific displacement-based boundary condition of ATAA wall found by ECG-gated CTA analysis with the flow-induced forces as determined by 2-way FSI analysis, but this poses remarkable technical challenges according to our experience with 2-way FSI. Moreover, model accuracy is determined by model design and quality of input data as well as validation against clinical gold-standard. Applications of 4D flow MRI for the study of ATAAs are promising to *in-vivo* assess the hemodynamic [25], but this technique is not a gold-standard procedure and requires technical expertise. The worse is for the assessment of the aortic wall stress since this cannot be measured *in-vivo*. Beyond technological development of computational modeling, and before these tools become established in routine clinical practice for risk stratification, the most immediate need is to show equivalence of computational results relative to invasive measurements through observational trials. Beyond this, efficacy must be demonstrated with studies, as the one here proposed, and then proved in large multicentre clinical trials.

Study Limitation

Several simplifications were made in our computational modeling approach. Material parameters and tissue thickness were assumed uniform for the entire aorta, although the ascending aorta and aortic root shows different biomechanical responses and thickness [26]. Material properties were not patient-specific but rather population-average values obtained from ex-vivo mechanical testing data reported by our group previously [19]. The methodology for the quantification of the displacement filed may have not fully considered the aortic twist because displacements were evaluated perpendicular to the aortic wall, although we estimated an error <10% [18]. Future studies will have to integrate patient-specific displacement-based boundary condition in 2-way FSI by investigating arbitrary Lagrangian-Eulerian (ALE) formulation or other FE techniques.

CONCLUSIONS

Computational modeling was adopted in this study to assess the effect of a compliant simulation of ATAA wall against a rigid wall simulation and the importance of adopting patient-specific displacement-based boundary conditions in FEA. This was assessed by comparison of hemodynamic and structural indices determined by less complex FEA and CFD analyses against a more sophisticated 2-way FSI modeling technique. Findings demonstrated that the stiff aneurysmal wall of patients with ATAA reduces the differences in the shear stress predictions between a rigid CFD simulation and a deformable 2-way FSI. When displacement boundary conditions are adopted to take into accounts for the aortic stretch and twist due to cardiac beating, differences in the IMS distribution can be observed between FEA and 2-way FSI modeling. Although spatial distribution of both WSS and IMS were found, Bland–Altman plots suggested a good agreement between modeling techniques. We cannot claim which one of computational technique is the gold-standard, because there is no standard to compare against, so that the efficacy of computational modeling techniques for risk stratification of ATAs must be further investigated.

ACKNOWLEDGMENTS

This work was supported by a "Ricerca Finalizzata" grant from the Italian Ministry of Health (GR-2011-02348129) to Salvatore Pasta, and by the Fondazione Ri.MED for research on aneurysm biomechanics.

REFERENCES

1. Isselbacher EM. Thoracic and abdominal aortic aneurysms. *Circulation*. 2005; 111: 816-28.
2. Davies RR, Goldstein LJ, Coady MA, et al. Yearly rupture or dissection rates for thoracic aortic aneurysms: Simple prediction based on size. *The Annals of Thoracic Surgery*. 2002; 73: 17-28.
3. Verma S, Siu SC. Aortic dilatation in patients with bicuspid aortic valve. *N Engl J Med*. 2014; 370: 1920-9.
4. Ince H, Nienaber CA. Etiology, pathogenesis and management of thoracic aortic aneurysm. *Nat Clin Pract Card*. 2007; 4: 418-27.
5. Fillinger MF, Marra SP, Raghavan ML, Kennedy FE. Prediction of rupture risk in abdominal aortic aneurysm during observation: Wall stress versus diameter. *J Vasc Surg*. 2003; 37: 724-32.
6. Nathan DP, Xu C, Gorman III JH, et al. Pathogenesis of acute aortic dissection: a finite element stress analysis. *Ann Thorac Surg*. 2011; 91: 458-63.
7. Nathan DP, Xu C, Plappert T, et al. Increased ascending aortic wall stress in patients with bicuspid aortic valves. *Ann Thorac Surg*. 2011; 92: 1384-9.
8. Martin C, Sun W, Elefteriades J. Patient-specific finite element analysis of ascending aorta aneurysms. *Am J Physiol Heart Circ Physiol*. 2015; 308: H1306-16.
9. Trabelsi O, Davis FM, Rodriguez-Matas JF, Duprey A, Avril S. Patient specific stress and rupture analysis of ascending thoracic aneurysms. *J Biomech*. 2015; 48: 1836-43.

10. Krishnan K, Ge L, Haraldsson H, et al. Ascending thoracic aortic aneurysm wall stress analysis using patient-specific finite element modeling of in vivo magnetic resonance imaging. *Interact Cardiovasc Thorac Surg*. 2015; 21: 471-80.

11. Kimura N, Nakamura M, Komiya K, et al. Patient-specific assessment of hemodynamics by computational fluid dynamics in patients with bicuspid aortopathy. *J Thorac Cardiovasc Surg*. 2017; 153: S52-S62 e3.

12. Rinaudo A, Pasta S. Regional variation of wall shear stress in ascending thoracic aortic aneurysms. *Proceedings of the Institution of Mechanical Engineers Part H, Journal of engineering in medicine*. 2014; 228: 627-38.

13. Pasta S, Gentile G, Raffa GM, et al. Three-dimensional parametric modeling of bicuspid aortopathy and comparison with computational flow predictions. *Artificial organs*. 2017.

14. Malvindi PG, Pasta S, Raffa GM, Livesey S. Computational fluid dynamics of the ascending aorta before the onset of type A aortic dissection. *European journal of cardio-thoracic surgery : official journal of the European Association for Cardio-thoracic Surgery*. 2016.

15. Numata S, Itatani K, Kanda K, et al. Blood flow analysis of the aortic arch using computational fluid dynamics(aEuro). *Eur J Cardio-Thorac*. 2016; 49: 1578-85.

16. Pasta S, Rinaudo A, Luca A, et al. Difference in hemodynamic and wall stress of ascending thoracic aortic aneurysms with bicuspid and tricuspid aortic valve. *Journal of biomechanics*. 2013; 46: 1729-38.

17. Pasta S, Gentile G, Raffa GM, et al. In Silico Shear and Intramural Stresses are Linked to Aortic Valve Morphology in Dilated Ascending Aorta. *European journal of*

vascular and endovascular surgery : the official journal of the European Society for Vascular Surgery. 2017.

18. Pasta S, Agnese V, Di Giuseppe M, et al. In Vivo Strain Analysis of Dilated Ascending Thoracic Aorta by ECG-Gated CT Angiographic Imaging. *Ann Biomed Eng*. 2017.
19. Pasta S, Phillippi JA, Tsamis A, et al. Constitutive modeling of ascending thoracic aortic aneurysms using microstructural parameters. *Medical engineering & physics*. 2016; 38: 121-30.
20. Kim HJ, Vignon-Clementel IE, Figueroa CA, et al. On Coupling a Lumped Parameter Heart Model and a Three-Dimensional Finite Element Aorta Model. *Annals of Biomedical Engineering*. 2009; 37: 2153-69.
21. Morbiducci U, Ponzini R, Rizzo G, et al. In vivo quantification of helical blood flow in human aorta by time-resolved three-dimensional cine phase contrast magnetic resonance imaging. *Ann Biomed Eng*. 2009; 37: 516-31.
22. Torii R, Oshima M, Kobayashi T, Takagi K, Tezduyar TE. Influence of wall elasticity in patient-specific hemodynamic simulations. *Comput Fluids*. 2007; 36: 160-8.
23. Reymond P, Crosetto P, Deparis S, Quarteroni A, Stergiopulos N. Physiological simulation of blood flow in the aorta: Comparison of hemodynamic indices as predicted by 3-D FSI, 3-D rigid wall and 1-D models. *Medical Engineering & Physics*. 2013; 35: 784-91.
24. Beller CJ, Labrosse MR, Thubrikar MJ, Robicsek F. Role of aortic root motion in the pathogenesis of aortic dissection. *Circulation*. 2004; 109: 763-9.

25. Barker AJ, Lanning C, Shandas R. Quantification of Hemodynamic Wall Shear Stress in Patients with Bicuspid Aortic Valve Using Phase-Contrast MRI. *Annals of Biomedical Engineering*. 2010; 38: 788-800.

26. Azadani AN, Chitsaz S, Mannion A, et al. Biomechanical properties of human ascending thoracic aortic aneurysms. *Ann Thorac Surg*. 2013; 96: 50-8.

Figure Legends

Figure 1. Flow patterns at systole in the aorta of a subset of bicuspid aortic valve patients (top) and tricuspid aortic valve patients (bottom).

Figure 2. Systolic wall shear stress (WSS) distribution for a subset of patients with bicuspid aortic valve on top and tricuspid aortic valve below.

Figure 3. Intramural stress (IMS) distribution at systole for a subset of patients with bicuspid aortic valve on top and tricuspid aortic valve below.

Figure 4. Helical Flow Index (HFI) and Pressure Index (PI) for CFD (Black) and 2-way FSI (White). *PI of CFD is significantly different from PI of 2-way FSI ($p < 0.05$).

Figure 5. Comparison of IMS and WSS distribution between FEA/CFD and 2-way FSI for one bicuspid aortic valve patients (left) and tricuspid aortic valve patients (right).

Table 1: Descriptive statistics of patient demographics, aortic diameters, and phenotypic classification of BAV

Patient	Valve	AoD (mm)	Age	Sex	TA flow (m/s)	Hypertension	AS	AI
(A)	RL-BAV	50.5	63	Female	2			1
(B)	AP-BAV	45.04	73	Male	1.6			
(C)	TAV	50.93	59	Male	1.3	Yes		
(D)	TAV	48.19	68	Female	1.4	Yes		
(E)	TAV	68.48	77	Male	2.6			
(F)	TAV	50.5	71	Male	1.5			2
(G)	AP-BAV	44.86	34	Male	1.2			1
(H)	TAV	46.71	65	Male	1.2			
(I)	TAV	51.68	64	Male	1.6			2
(J)	AP-BAV	48.81	65	Male	2.6	Yes	2	1
(K)	TAV	32.42	57	Male	0.88			1

Note: AP = fusion of the right and left coronary cusp; RL = fusion of the right and non-coronary cusp; AoD = aortic diameter; TA = transaortic jet velocity; AS = aortic stenosis; AI = aortic regurgitation; 1= minimal; 2 = moderate

Table 2: Pearson correlation coefficient between FEA/CFD analyses and 2-way FSI for the investigated hemodynamic and structural parameters (p-value in brackets)

	Pearson Correlation Coefficient				
Location	**Pressure**	**WSS**	**IMS**	**PI**	**HFI**
STJ	-0.0301 (0.930)	-0.0282 (0.934)	-0.110 (0.747)	-0.469 (0.145)	-0.209 (0.537)
AA Middle	0.00258 (0.994)	-0.0236 (0.945)	-0.0168 (0.961)		
AA Distal	-0.296 (0.376)	-0.230 (0.496)	0.264 (0.416)		

Table 3: Spearman correlation coefficient between FEA/CFD analyses and 2-way FSI for the investigated hemodynamic and structural parameters (p-value in brackets)

	Spearman Correlation Coefficient				
Location	**Pressure**	**WSS**	**IMS**	**PI**	**HFI**
STJ	0.218 (0.502)	0.105 (0.734)	-0.136 (0673)	-0.473 (0.132)	-0.0456 (0.881)
AA Middle	0.209 (0.520)	-0.169 (0.595)	0.209 (0.520)		
AA Distal	-0.323 (0.310)	-0.0755 (0.818)	0.0967 (0.777)		

Figure 1

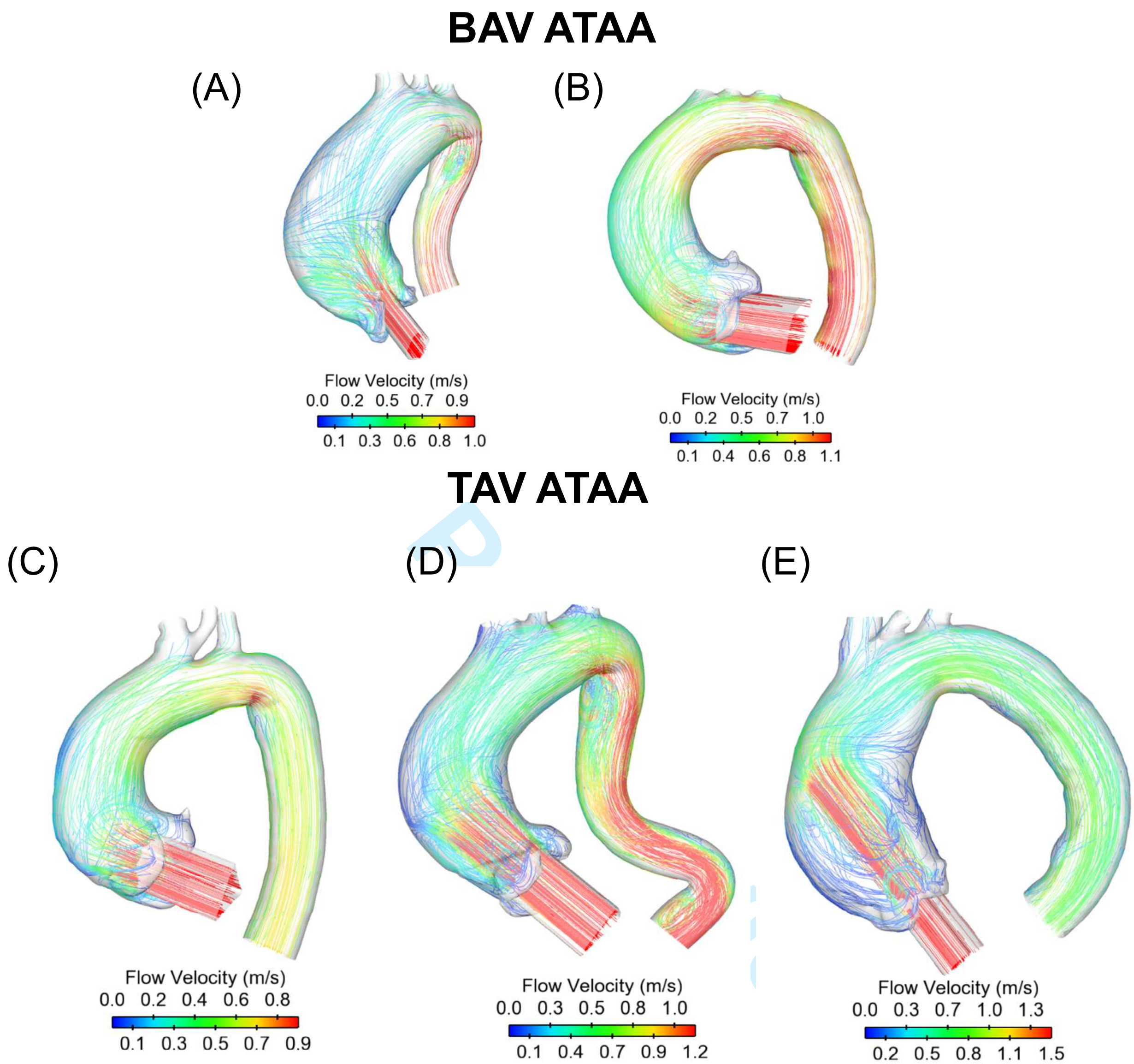
BAV ATAA
(A)
(B)
Flow Velocity (m/s)
0.0 0.2 0.5 0.7 0.9
0.1 0.3 0.6 0.8 1.0
Flow Velocity (m/s)
0.0 0.2 0.5 0.7 1.0
0.1 0.4 0.6 0.8 1.1
TAV ATAA
(C)
(D)
(E)
Flow Velocity (m/s)
0.0 0.2 0.4 0.6 0.8
0.1 0.3 0.5 0.7 0.9
Flow Velocity (m/s)
0.0 0.3 0.5 0.8 1.0
0.1 0.4 0.7 0.9 1.2
Flow Velocity (m/s)
0.0 0.3 0.7 1.0 1.3
0.2 0.5 0.8 1.1 1.5

Figure 2

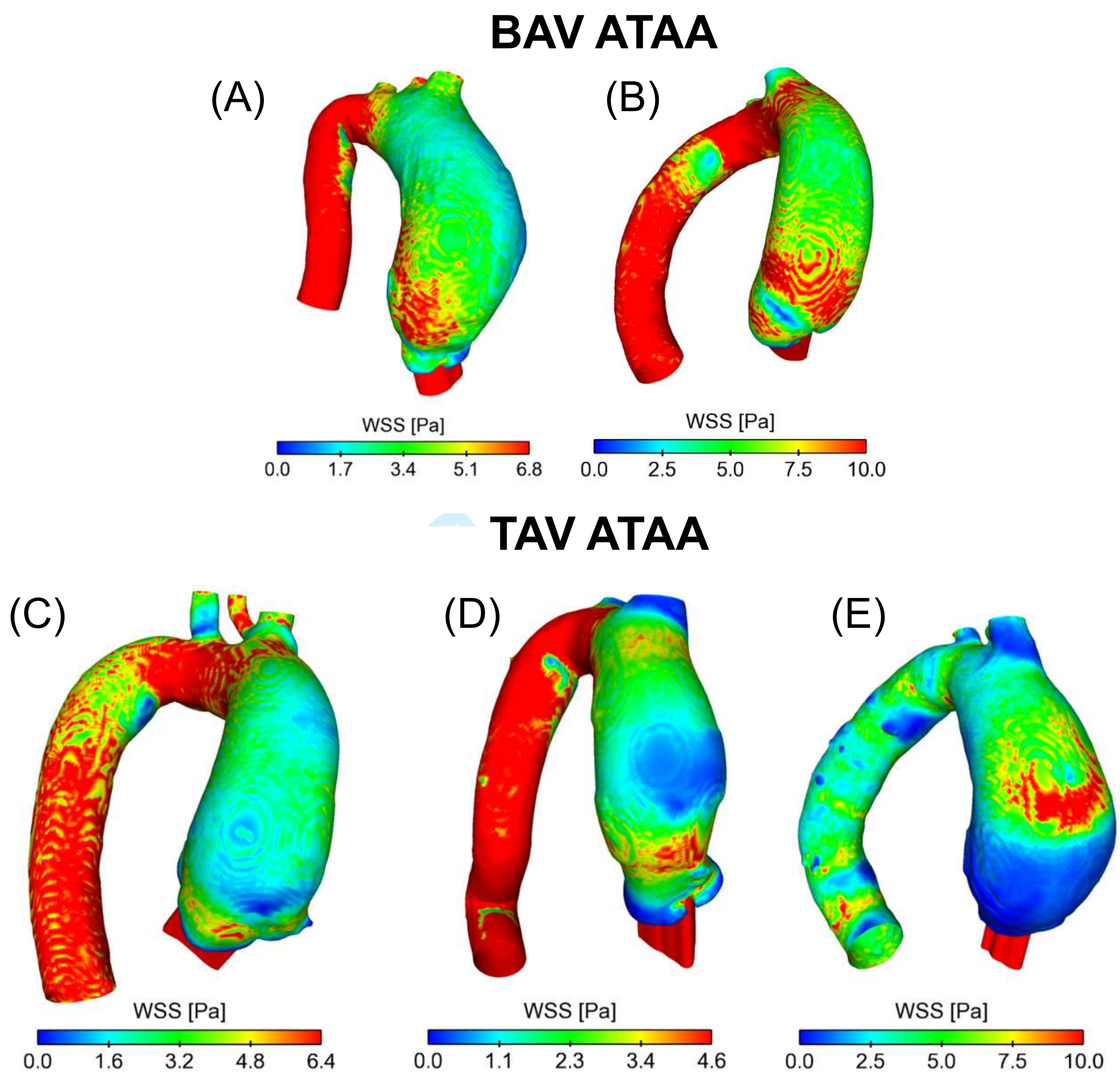
BAV ATAA
(A)
(B)
WSS [Pa]
0.0 1.7 3.4 5.1 6.8
WSS [Pa]
0.0 2.5 5.0 7.5 10.0
TAV ATAA
(C)
(D)
(E)
WSS [Pa]
0.0 1.6 3.2 4.8 6.4
WSS [Pa]
0.0 1.1 2.3 3.4 4.6
WSS [Pa]
0.0 2.5 5.0 7.5 10.0

Figure 3

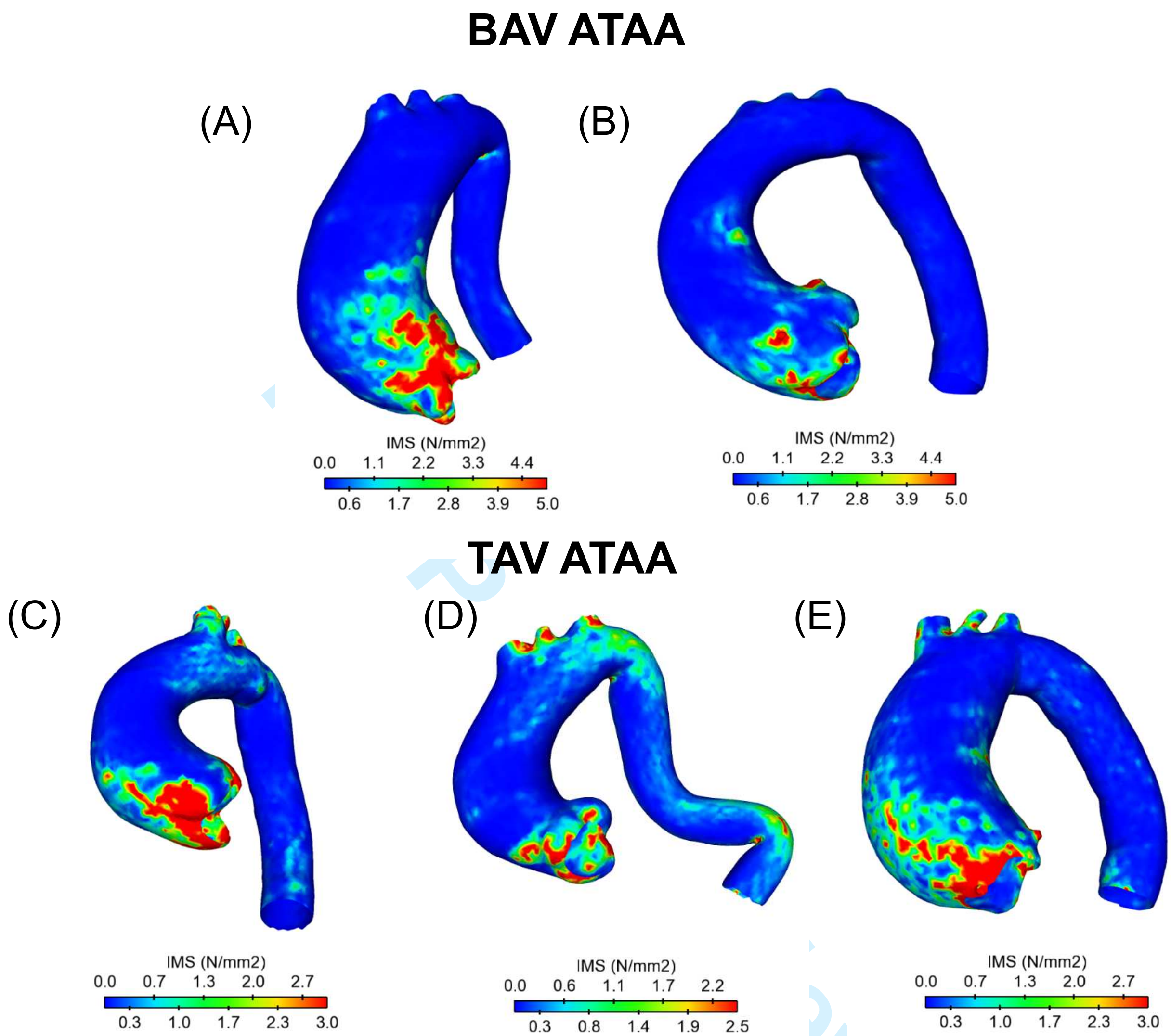
BAV ATAA
(A)
(B)
IMS (N/mm2)
0.0 1.1 2.2 3.3 4.4
0.6 1.7 2.8 3.9 5.0
IMS (N/mm2)
0.0 1.1 2.2 3.3 4.4
0.6 1.7 2.8 3.9 5.0
TAV ATAA
(C)
(D)
(E)
IMS (N/mm2)
0.0 0.7 1.3 2.0 2.7
0.3 1.0 1.7 2.3 3.0
IMS (N/mm2)
0.0 0.6 1.1 1.7 2.2
0.3 0.8 1.4 1.9 2.5
IMS (N/mm2)
0.0 0.7 1.3 2.0 2.7
0.3 1.0 1.7 2.3 3.0

26

Figure 4

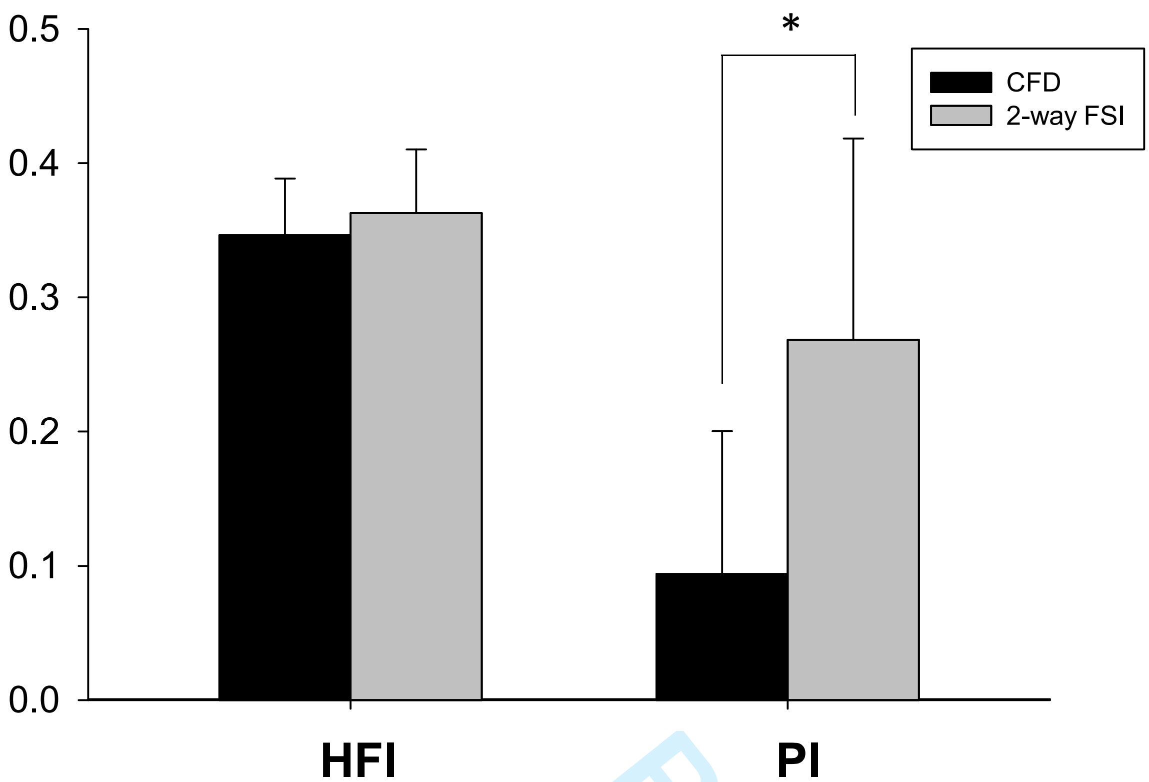

Figure 5

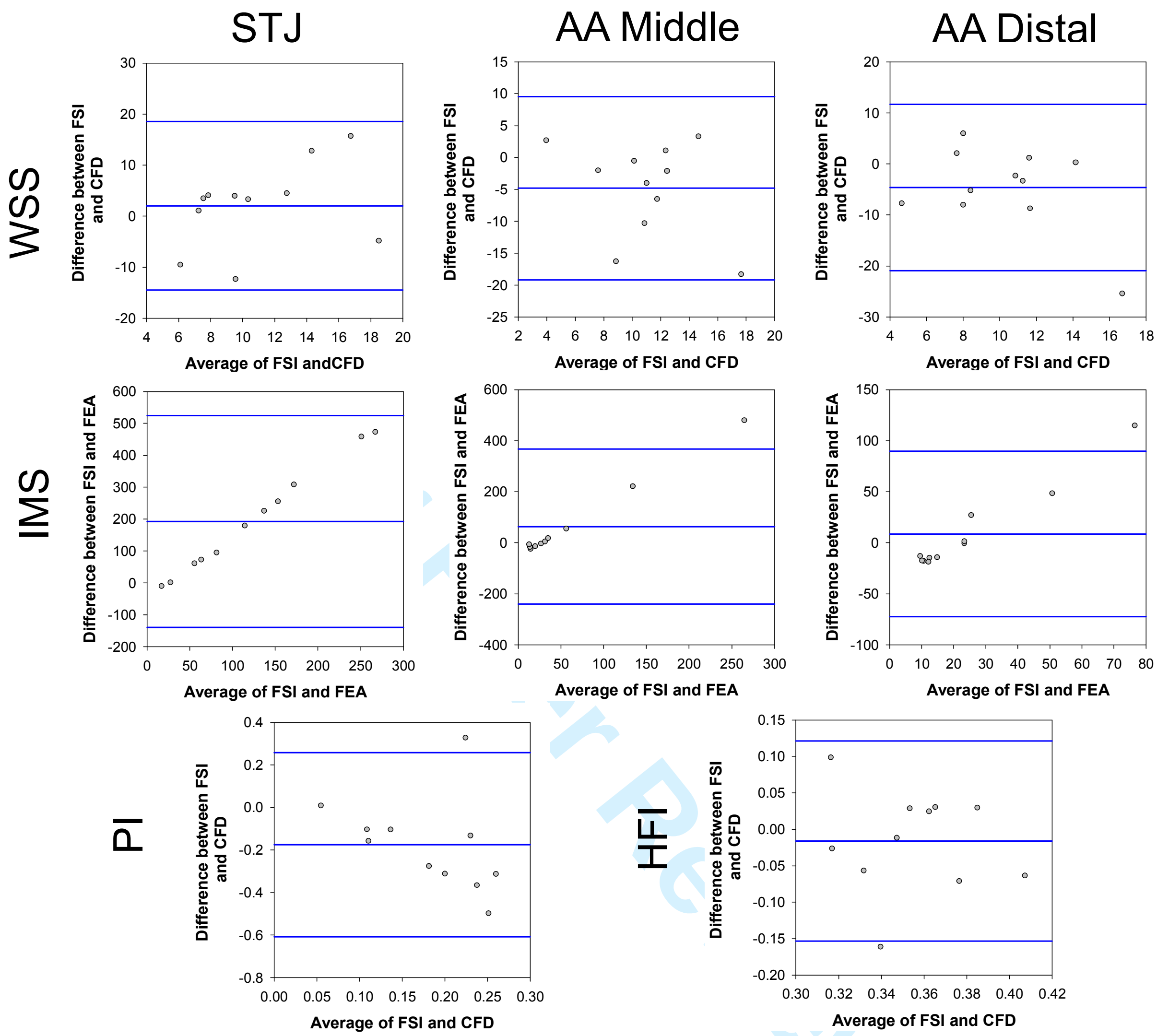
STJ
AA Middle
AA Distal
WSS
IMS
PI
HFI
Difference between FSI and CFD
Difference between FSI and FEA
Average of FSI andCFD
Average of FSI and CFD
Average of FSI and FEA

28

Figure 6

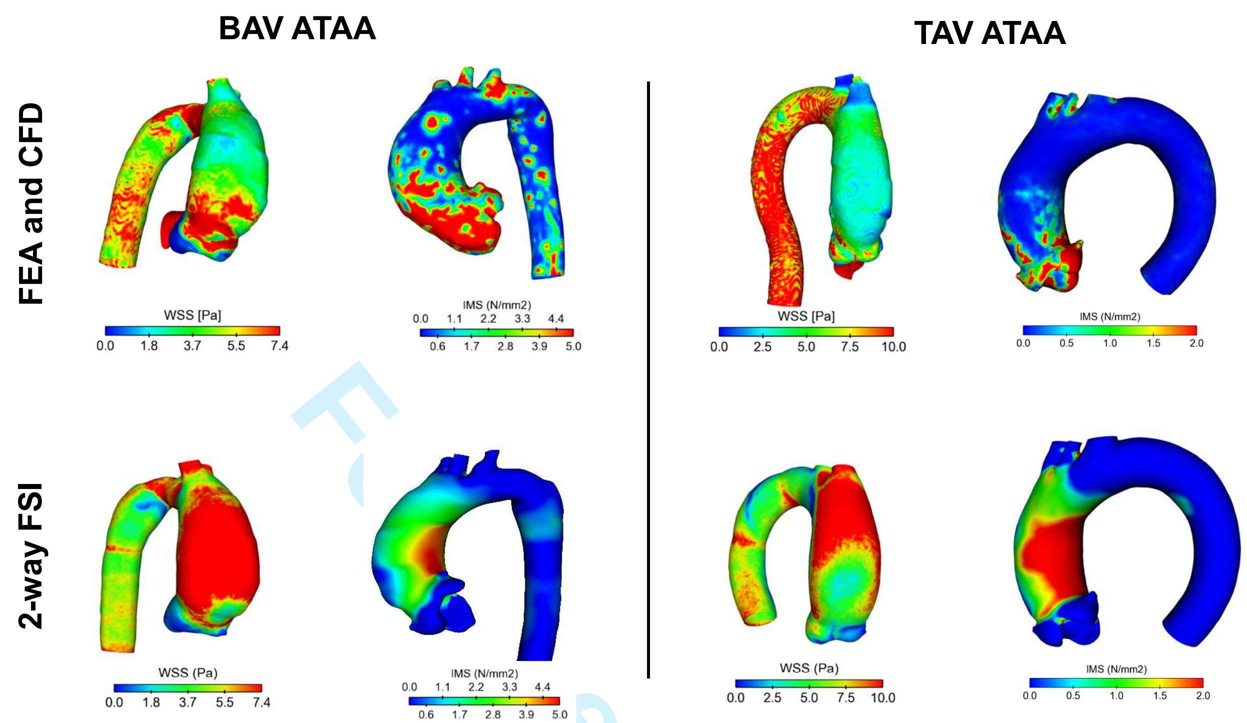
BAV ATAA
TAV ATAA
FEA and CFD
2-way FSI
WSS [Pa]
0.0 1.8 3.7 5.5 7.4
IMS (N/mm2)
0.0 1.1 2.2 3.3 4.4
0.6 1.7 2.8 3.9 5.0
WSS [Pa]
0.0 2.5 5.0 7.5 10.0
IMS (N/mm2)
0.0 0.5 1.0 1.5 2.0
WSS (Pa)
0.0 1.8 3.7 5.5 7.4
IMS (N/mm2)
0.0 1.1 2.2 3.3 4.4
0.6 1.7 2.8 3.9 5.0
WSS (Pa)
0.0 2.5 5.0 7.5 10.0
IMS (N/mm2)
0.0 0.5 1.0 1.5 2.0